Global dendritic calcium spikes in mouse layer 5 low threshold spiking interneurones: implications for control of pyramidal cell bursting

Jesse H. Goldberg, Clay O. Lacefield and Rafael Yuste

Department Biological Sciences, Columbia University, New York, NY 10027, USA

Interneuronal networks in neocortex underlie feedforward and feedback inhibition and control the temporal organization of pyramidal cell activity. We previously found that lower layer neocortical interneurones can reach action potential threshold in response to the stimulation of a single presynaptic cell. To better understand this phenomenon and the circuit roles of lower layer neocortical interneurones, we combined two-photon calcium imaging with whole cell recordings and anatomical reconstructions of low threshold spiking (LTS) interneurones from mouse neocortex. In both visual and somatosensory cortex, LTS interneurones are somatostatin-positive, concentrated in layer 5 and possess dense axonal innervation to layer 1. Due to the LTS properties, these neurones operate in burst and tonic modes. In burst mode, dendritic T-type calcium channels boosted small synaptic inputs and triggered low threshold calcium spikes, while in tonic mode, sodium-based APs evoked smaller calcium influxes. In both modes, the entire dendritic tree of LTS interneurones behaved as a 'global' single spiking unit. This, together with the fact that synaptic inputs to layer 5 LTS cells are facilitating, and that their axons target the dendritic region of the pyramidal neurones where bursts are generated, make these neurones ideally suited to detect and control burst generation of individual lower layer pyramidal neurones.

(Resubmitted 17 March 2004; accepted after revision 12 May 2004; first published online 14 May 2004)
Corresponding author J. H. Goldberg: Department of Biological Sciences, Columbia University, New York, NY 1002, USA. Email: jhg24@columbia.edu

Neocortical neurones have extensive dendritic arbors which receive inputs from presumably thousands of other neurones (Cajal, 1899). It is generally believed that, in pyramidal neurones and fast spiking interneurones, the summed activation of multiple presynaptic excitatory inputs is necessary to drive APs, suggesting that both excitatory and inhibitory streams of the neocortex employ sparse, distributed encoding (Abeles, 1991; Rolls & Treves, 1998). In agreement with this, in most classes of interneurones, unitary synaptic inputs cannot generate suprathreshold activation, perhaps due to small unitary EPSP amplitudes (Porter *et al.* 1998; Angulo *et al.* 1999; Rozov *et al.* 2001). Moreover, in upper layers (2/3) of mouse visual cortex, we have recently shown that in parvalbumin-positive fast-spiking (FS) and calretinin-positive irregular spiking (IS) interneurones an A-type potassium current restricts AP backpropagation (Goldberg *et al.* 2003*b*). This high expression of dendritic potassium currents could further dampen excitation of individual inputs (Fricker & Miles, 2000).

However, it has been reported that a single presynaptic pyramidal neurone can evoke suprathreshold firing in some types of interneurones (Miles & Wong, 1983; Markram *et al.* 1998; Kaiser *et al.* 2004). In our optical study of intralaminar connections of mouse layer 5, we recently found that single-axon inputs to layer 5 LTS interneurones could generate postsynaptic spikes (Kozloski *et al.* 2001). Furthermore, sodium spikes generated from these unitary inputs appeared to be preceded by plateau potentials, suggesting that dendritic calcium channels amplified synaptic inputs. We were surprised by the strength of the unitary connections in these circuits, and wondered what mechanisms produced them and what function they may serve. Because it has been recently shown that, like pyramidal neurones (Johnston *et al.* 1996; Yuste & Tank, 1996), dendrites of GABAergic interneurones express voltage-gated channels (Martina *et al.* 2000; Kaiser *et al.* 2001; Goldberg *et al.* 2003*b*), we wondered if active dendritic conductances were involved in boosting small synaptic inputs to enable

 DOI: 10.1113/jphysiol.2004.064519

suprathreshold sensitivity to unitary connections in specific interneuronal classes.

To study this question we used a combination of imaging, electrophysiological experiments and anatomical reconstruction. We find that, in both visual and somatosensory cortices, LTS interneurones were somatostatin-positive Martinotti cells, concentrated in layer 5 with dense axonal innervation to layer 1. As in thalamic relay and reticular neurones (Jahnsen & Llinas, 1984; Crunelli *et al.* 1989), LTS interneurones operate in burst and tonic firing modes. In addition, due to the regenerative propagation of sodium-based APs and I_T-triggered low threshold spikes through vast territories of the dendritic tree, LTS interneurones behave as all-or-none spiking units, apparently unable to generate local calcium signals. Because of their synaptic properties and their axonal distribution, we propose that layer 5 LTS interneurones throughout the neocortex detect and control bursting behaviour in populations of deep layer pyramids.

Methods

Slice preparation and electrophysiology

Experiments were carried out in accordance with the NIH Guide for the Care and Use of Laboratory Animals (NIH publication no. 86-23, revised 1987) and with the Society for Neuroscience 1995 Statement (http://www.jneurosci.org/misc/itoa.shtml). Coronal slices of primary visual or somatosensory cortex were made from P13–17 C57BL/6mice. Animals were anaesthetized with ketamine–xylazine (50 and 10 mg kg^{-1}). After decapitation, brains were rapidly removed and transferred into ice-cold cutting solution containing (mM): 222 sucrose, 27 $NaHCO_3$, 2.5 KCl, 1.5 NaH_2PO_4, bubbled with 95% O_2–5% CO_2 to pH 7.4. Brains were cooled for at least 2 min and 300-μm-thick slices were prepared with a Vibratome (VT1000, Leica, Germany). Slices were then transferred to a heated solution (35°C) containing (mM) 126 NaCl, 3 KCl, 1.1 NaH_3PO_4, 26 $NaHCO_3$, 1 $CaCl_2$, 3 $MgSO_4$, bubbled with 95% O_2–5% CO_2 to pH 7.4, which cooled down in the next 30 min to room temperature. Slices were transferred to the imaging chamber 1–7 h after cutting. Artificial cerebral spinal fluid (ACSF) during experiments contained (mM): 126 NaCl, 3 KCl, 1.1 NaH_3PO_4, 26 $NaHCO_3$, 3 $CaCl_2$, 1 Mg_2SO_4, bubbled with 95% O_2–5% CO_2 to pH 7.4. All experiments were performed at 37°C. Whole cell recordings from non-pyramidal cells in layer 2/3 were obtained with patch clamp amplifier (Axoclamp 2B, Axon Instruments, Union City, CA, USA; or BVC-700, Dagan Corp., Minneapolis, MN, USA). Mechanisms of backpropagation or synaptic calcium influx were explored with several drugs (Sigma), including cyclopiazonic acid (CPA) (50 μM), 6,7-dinitro-quinoxaline-2,3-dione (DNQX) (20 μM), D(−)-2-amino-5-phosphonopentanoic acid (D-APV) (50–100 μM), $NiCl_2$ (20 μM), and TTX (1 μM). Trolox (100 μM, Aldrich) was added to ACSF to reduce phototoxicity. Neurones were stimulated synaptically using an extracellular pipette filled with 500 μM Alexa-488 dextran (Molecular Probes, Eugene, OR, USA) in ACSF. Tips of stimulation pipettes were bent by about 70 deg with a microforge (Narishige, Japan). This allowed positioning of the stimulation pipette perpendicular to the slice surface. In order to achieve local subthreshold stimulation it was necessary to place glass electrodes in the immediate vicinity (< 15 μm) of the dendrite of interest, and trigger with brief (100 μs) shocks at 0.2–1 V.

Two-photon imaging

Cells were filled via patch pipette with 100 μM Fluo- 4 (Molecular Probes). Pipette solution contained (mM): 130 potassium methylsulphonate, 5 KCl, 5 NaCl, 10 Hepes, 2.5 Mg-ATP, 0.3 GTP and 0.03% biocytin and was titrated to pH 7.3. Following break-in, we waited for 20 min before imaging to ensure that dendrites filled with indicator. Imaging was performed with a custom-made two-photon laser scanning microscope (Majewska *et al.* 2000), consisting of a modified Fluoview (Olympus, Melville, NY, USA) confocal microscope with a Ti:sapphire laser providing 130 fs pulses at 75 MHz (Mira, Coherent, Santa Clara, CA, USA), and pumped by a solid-state source (Verdi, Coherent). A 60×, 0.9 numerical aperture water immersion objective (IR1, Olympus) was used. Fluorescence was detected with photo multiplier tubes (HC125-02, Hamamatsu, Hamamatsu City, Japan) in external whole-area detection mode, and images were acquired and analysed with Fluoview (Olympus) software. Images of dendrites were acquired at 10× digital zoom, resulting in a nominal spatial resolution of 30 pixels μm^{-1} and at a time resolution of 12.64 ms per point (79 Hz) in line scan mode.

Analysis

Fluorescence levels of calcium measurements were analysed using ImageJ software (NIH, Bethesda, MD, USA). Time courses were analysed using the Igor analysis package (Wavemetrics, Lake Oswego, OR, USA). Calcium

signals during AP generation were detected in line scan mode with a temporal resolution of 79 Hz, and the relative change of fluorescence of baseline (from 400 ms prior to AP generation) ($\Delta F/F$) was used as indicator for the change in calcium. Between 5 and 15 line scans were typically averaged to generate $\Delta F/F$ transients during action potentials. Decay kinetics were fitted using single exponential fitting algorithms of Igor. For intergroup comparisons, two-sided Student's t tests were used, and data are presented as means ± standard deviation. Distances from the soma were measured from the site of dendritic imaging to the location where the parent dendrite emerged from the soma.

Histology

Visualization of biocytin-stained cells was performed as described by Kozloski *et al.* (2001). Three-dimensional light microscopic reconstructions were carried out using Neurolucida and Neuro Explorer acquisition and analysis packages (MicroBrightfield, Colchester, VT, USA) with a 100× oil objective.

Results

Somatostatin-positive LTS Martinotti cells in layer 5 of mouse visual and somatosensory cortices

We performed combined imaging–electrophysiological–anatomical experiments on 18 LTS cells from mouse primary visual and somatosensory cortices. We should emphasize that not all interneurones which have previously been termed LTS, for example, those in layer 4 of rat somatosensory cortex (Gibson *et al.* 1999; Beierlein *et al.* 2000; Deans *et al.* 2001; Amitai *et al.* 2002; Beierlein *et al.* 2003), appear to generate rebound bursts and to operate in burst and tonic modes. Thus those cells may represent a distinct subclass from the ones we consider here. To clarify our nomenclature, we strictly defined 'true' LTS interneurones as cells which generated rebound bursts following somatic hyperpolarization (Fig. 1*A*) (Kawaguchi & Kubota, 1996; Kawaguchi & Kondo, 2002). In thalamic neurones, these rebound bursts are triggered by T-type calcium channels (Crunelli *et al.* 1989; Kim *et al.* 2001), suggesting that LTS interneurones express them at high densities. We found LTS neurones primarily in layer 5. Moreover, of our sample of over 100 supragranular interneurones recorded in mouse visual cortex, none exhibited rebound bursts, the defining parameter of the LTS phenotype (Goldberg *et al.* 2003*b*).

Depending on the membrane potential, LTS interneurones operated in two distinct modes. At hyperpolarized potentials (-77.1 ± 6.1 mV, $n = 18$), sustained or transient (< 5 ms) depolarizations caused a burst of action potentials riding on a low threshold spike with a prolonged afterdepolarization (Fig. 1*A* and *B*). This physiological signature of the LTS was also observed during rebound bursts following hyperpolarizations from rest (Fig. 1*A*, Supplementary material). On the other hand, at depolarized potentials (-56.0 ± 3.1 mV, $n = 18$), the low threshold spike and related burst were absent. Together, these results suggest steady state voltage-dependent inactivation of I_T (Fox *et al.* 1987). At resting membrane potentials (65.5 ± 4.4 mV, $n = 18$), 14/18 LTS interneurones generated low threshold spikes, suggesting that in the absence of significant background activity, LTS interneurones are in burst mode.

We took advantage of somatostatin (SST) expression in LTS interneurones (Kawaguchi & Kubota, 1996; Cauli *et al.* 1997; Kawaguchi & Kondo, 2002) to target them using homozygotic GFP-SST mice (Fig. 1*B*). Over half of the SST^+ cells in layer 5 had LTS phenotype ($n = 7/13$), and the rest were regular-spiking adapting non-pyramidal cells and are not included in this study. Because these SST-positive interneurones were morphologically and physiologically identical to LTS interneurones from wild-type mice, we pooled them together for this study.

Anatomically LTS cells had dendrites which were mostly compact and limited to deep layers. On the other hand, their axons were prolific and densely innervated layer 1, characteristic of classical Martinotti cells (Fig. 1*C*) (Lorente De Nó, 1922; Ruiz-Marcos & Valverde, 1970; Fairen *et al.* 1984; Braitenberg & Schüzt, 1991). We concluded that these LTS interneurones from mouse neocortex are Martinotti cells.

Low threshold spikes dominate intrinsic dendritic calcium dynamics

We were interested in understanding how the LTS behaviour affected intrinsic dendritic calcium dynamics during action potential (AP) backpropagation. In neocortical layers 2/3, AP backpropagation in somatostatin-positive bitufted interneurones causes instantaneous calcium accumulations (Kaiser *et al.* 2001), and in parvalbumin-positive FS and calretinin-positive IS cells AP backpropagation is spatially controlled by Ia-type potassium channels (Goldberg *et al.* 2003*c*). However, owing to their potentially high expression of low-voltage-activated (LVA) calcium channels, calcium electrogenesis in dendrites of LTS neurones could dramatically differ from the non-LTS interneurones (Gee *et al.* 2001; Kaiser *et al.* 2001; Goldberg *et al.* 2003*a*,*b*,*c*; Kaiser *et al.* 2004; Rozsa *et al.* 2004).

We triggered APs in burst or tonic modes and examined the dendritic calcium influx as a function of distance from the soma. Dendritic calcium accumulations were dominated by low threshold spikes, which could be generated exclusively in burst mode at hyperpolarized potentials (-77.1 ± 6.1 mV, $n = 18$) (Fig. 2). Transient somatic current injections (< 5 ms) caused a burst of sodium-based action potentials riding on an LTS which significantly outlasted the duration of the injected current (Fig. 2*B*). The amplitude of the calcium transient during the LTS was increased at distal dendrites, although this trend was only significant compared to the peak signal at the soma (Fig. 2*G*), suggesting that the low threshold channels underlying the LTS were expressed at higher densities at distal dendrites.

The same transient current injection that caused an LTS and burst of APs at hyperpolarized potentials caused a single AP at depolarized potentials (-56.0 ± 3.1 mV, $n = 18$) (Fig. 2*C*). These single APs also backpropagated into the dendritic tree, but caused significantly smaller calcium influxes than the LTS at all distances from the soma (Fig. 2*C*–*G*) (ratio $(\Delta F/F_{AP})/(\Delta F/F_{LTS})$ for soma was 0.31 ± 0.19, $P < 0.05$; proximal ($< 40\ \mu$m), 0.35 ± 0.18, $P < 0.05$; intermediate (41–80 μm), 0.17 ± 0.05, $P < 0.001$; distal, 0.17 ± 0.15, $P < 0.001$; $n = 18$).

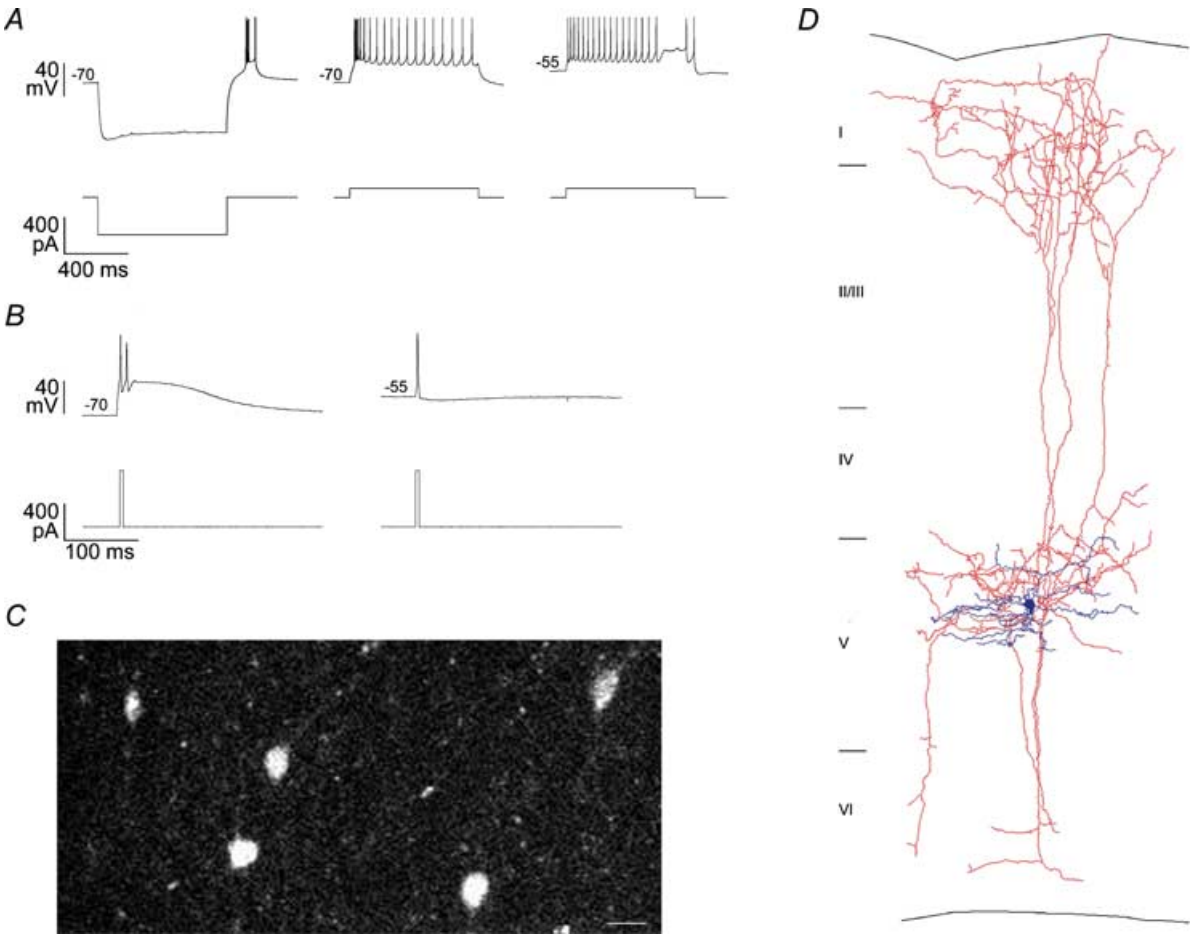

Figure 1. Low threshold spiking somatostatin-positive layer 5 cells
A, left, voltage response (top) of a representative somatostatin-positive layer 5 LTS interneurone cell to hyperpolarizing current injection (bottom). Note the rebound LTS burst after release from hyperpolarization. Firing pattern was generated with cell held at -70 mV, middle, and -55 mV, right. Note that the bursting firing pattern at -70 mV is absent at -55 mV. *B*, left, delivery of transient (4 ms) depolarizing current (bottom), at -70 mV resulted in an LTS burst (top), which outlasted the duration of the current injection. Right, the same current injection at -55 mV evoked a single spike. *C*, somatostatin-positive cells from layers 4–5 of the visual cortex of a somatostatin–GFP transgenic mouse. Scale bar = 20 μm. *D*, biocytin reconstruction of a layer 5 LTS Martinotti cell. Note the local dendritic arborization (dark), and the axons ascending to layer 1 (light).

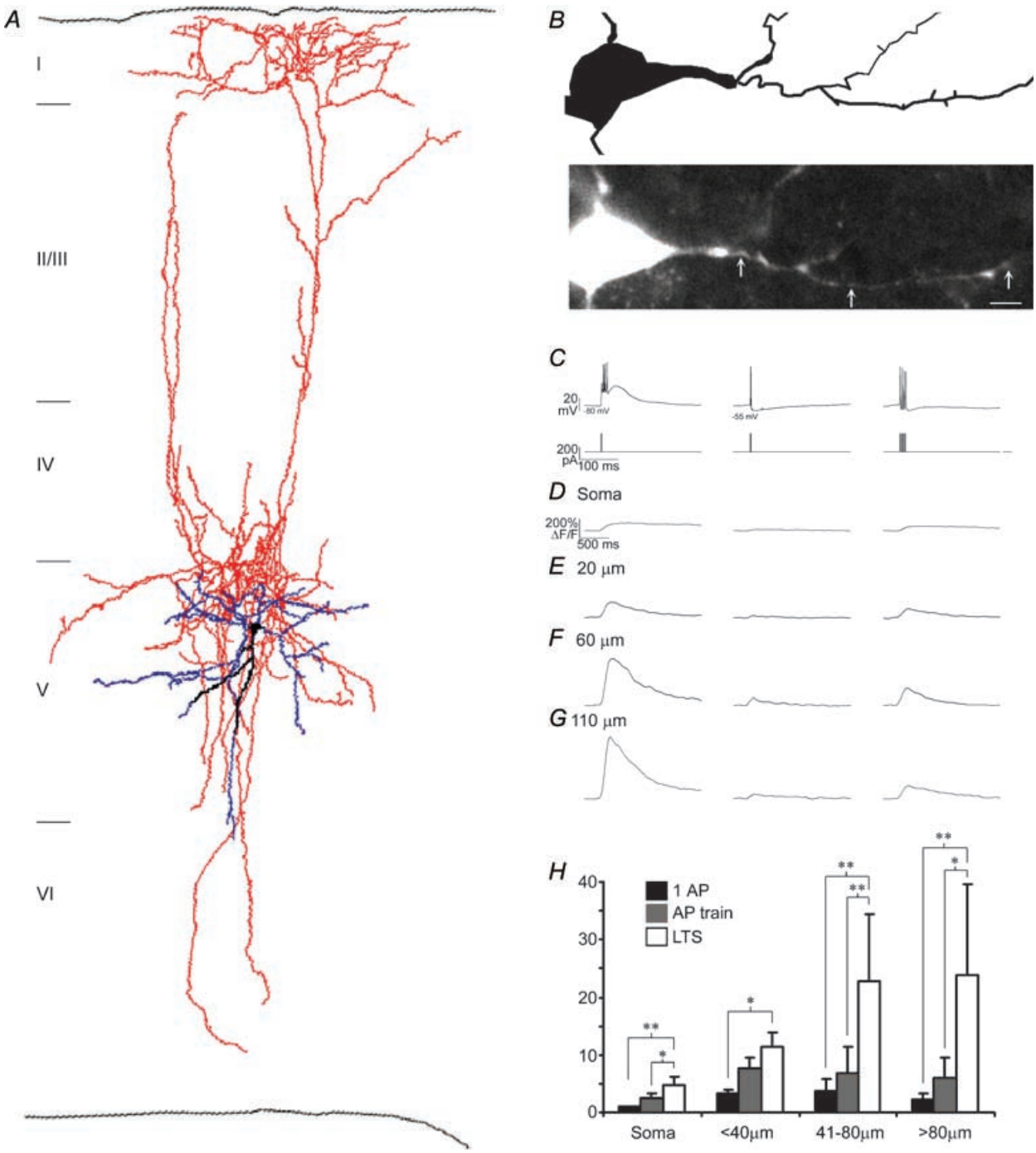

Figure 2. Low threshold spikes dominate dendritic calcium dynamics
A, anatomical reconstruction of layer 5 LTS cell. *B*, basal dendritic arborization from reconstructed in *A* (top), and *z*-projection of the identical cellular region acquired during fluorescence imaging (bottom). Arrows indicate dendritic sites where line scans were performed at an additional 10× zoom. Scale bar = 10 μm. *C*, voltage responses (top) to 4 ms somatic current injections (bottom). Note that the envelope of the low threshold spike recruited at the hyperpolarized potential (−75 mV) outlasted the duration of the current injection. Calcium transients during the stimulation regimes outlined in *C* acquired at the soma (*D*), and 20 μm, 60 μm, and 110 μm from the soma (*E*–*G*), respectively. The LTS-associated calcium signal evoked in burst mode (−80 mV) dominated over single APs or AP trains evoked in tonic mode (−55 mV). The number of APs evoked in a train was matched to the number of APs generated during the LTS burst, and ranged from 2 to 4 ($n = 18$). Note the different time scales in *B* and *C*–*F*. *H*, pooled data, demonstrating the dominance of the dendritic calcium signal during the LTS. $^{*}P < 0.005$; $^{**}P < 0.001$.

To compare the LTS dendritic calcium signals to those evoked by backpropagating APs alone, we generated trains of APs in tonic mode and found that calcium signals during LTS-triggered AP bursts were also significantly larger than AP trains containing an equal number of APs generated by the burst (Fig. 2*C*–*G*). This finding was statistically significant at all dendritic regions except at proximal dendrites, again suggesting that the LTS is more robust distally (ratio $(\Delta F/F_{\mathrm{APtrain}})/(\Delta F/F_{\mathrm{LTS}})$: soma, 0.56 ± 0.21, $P < 0.05$; proximal, 0.70 ± 0.26, n.s.; intermediate 0.23 ± 0.10, $P < 0.05$; distal 0.34 ± 0.24, $P < 0.05$; $n = 18$).

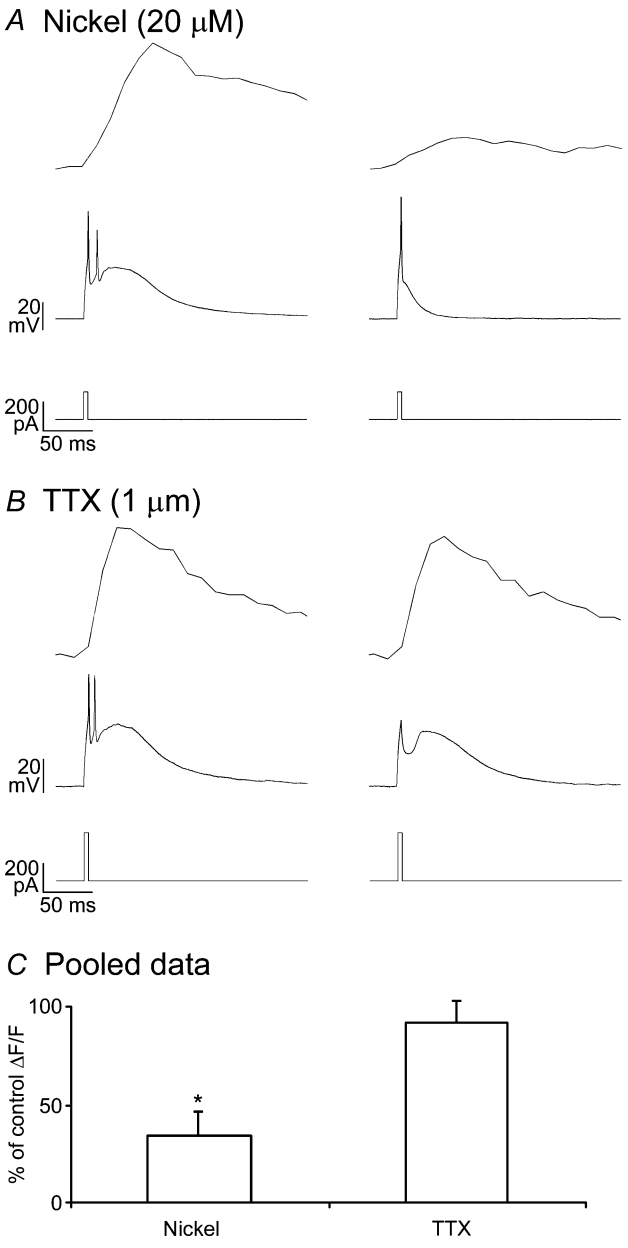

Figure 3. T-type calcium channels trigger regeneratively propagated dendritic spikes and cause calcium influx in distal dendrites

A, low concentrations of nickel (20 μM) significantly reduced dendritic calcium influx and the size and duration of the LTS. Calcium transients (top) during the LTS (middle) evoked during 4 ms somatic current injections (bottom) in control (left) and after addition of 20 μM nickel (right). *B*, data plotted as in *A* in the presence of TTX. Both transients were acquired from distal dendrites (> 80 μm). *C*, 20 μM Ni^{2+} ($n = 3$) significantly reduced dendritic calcium transients, while blockade of sodium channels with 1μM TTX ($n = 3$) did not.

Low threshold spikes regeneratively propagate through the dendritic tree

Our finding that LTS-associated dendritic calcium accumulations were larger than those produced by an equal number of APs suggested that the LTS itself provided a distinct dendritic calcium influx (Fig. 2*C*–*G*). To test whether LVA calcium channels triggered the LTS and were thus the major source of dendritic calcium, we compared calcium accumulations before and after addition of 20 μM nickel to reduce T- and R-type calcium channel activity (Fox *et al.* 1987; Foehring *et al.* 2000; Sochivko *et al.* 2003). Indeed, low nickel significantly reduced both the low threshold spike and its associated dendritic calcium signal (% $\Delta F/F$ reduction: $67 \pm 12\%$, $P < 0.05$, $n = 3$) (Fig. 3*A*).

Interestingly, most of the calcium influx during LTS generation was synchronous with the slow LTS-driven depolarization, and not with the fast sodium-based APs (Fig. 3*A* and *B*). We wondered if low threshold spikes triggered by somatic current injections could regeneratively propagate in the absence of sodium channels. Indeed, addition of TTX (1 μM) to block sodium channels did not have a significant effect on LTS-associated dendritic calcium signals (Fig. 3*B* and *C*). Thus, similar to conduction of I_{T}-based action potentials through cardiac muscle fibres (Hermsmeyer, 1998), low threshold spikes regeneratively propagated through LTS cell dendrites, even in the absence of functional sodium channels.

Short-term facilitating synapses on LTS interneurone dendrites

In three populations of supragranular interneurones, local synaptic stimulation of multiple synapses converging to an individual dendritic compartment causes NMDA receptor-dominated calcium accumulations restricted in space to individual dendritic domains (~10 μm) (Goldberg *et al.* 2003*b*). In addition, in fast spiking interneurones, activation of individual synapses containing calcium-permeable AMPA receptors caused much smaller calcium microdomains (< 1 μm) (Goldberg *et al.* 2003*a*). In these studies, we achieved local synaptic excitation

by delivering brief (100 μs), low intensity (1–3 V), single shocks through a stimulation electrode placed immediately adjacent ($< 15\ \mu$m) to the dendritic compartment of interest (see methods).

To investigate synaptically triggered dendritic calcium influxes in LTS cells, we positioned stimulation electrodes as previously described, immediately adjacent ($< 15\ \mu$m) to distal dendrites. We found that the synaptic behaviour of LTS cells dramatically differed from neocortical pyramidal neurones and of all of the interneurone subtypes previously examined (Schiller *et al.* 2000; Goldberg *et al.* 2003*a*,*c*). Single shocks, even at maximal attainable intensities (10 V) and at increased durations (300 μs), failed to elicit significant depolarization from either burst or tonic modes. Further, single shocks never caused detectable calcium signals, even at the distal dendrite adjacent to the stimulation electrode ($n = 10/10$).

Excitatory synapses on layer 2–4 neocortical SST interneurones show short-term facilitation (Reyes *et al.* 1998; Gibson *et al.* 1999; Kaiser *et al.* 2004). Thus, to generate an excitatory drive, we stimulated with trains of synaptic inputs (3 shocks at 40 or 100 Hz), and confirmed this facilitation for layer 5 SST LTS cells (2nd/1st EPSP amplitude $= 3.7 \pm 4.2$, $P < 0.05$, $n = 10$) (Fig. 4*B*). Surprisingly, LTS cells did not exhibit calcium influx during trains of synaptic stimulation which were subthreshold for either the low threshold spike at hyperpolarized potentials or sodium-based APs at depolarized potentials ($n = 10/10$) (Fig. 5). The only manner to synaptically evoke dendritic calcium signals in LTS cells was to deliver suprathreshold trains of synaptic input. Importantly, every time an LTS was triggered, it provided sufficient depolarization to recruit a burst of sodium based action potentials.

Since EPSP trains were strongly facilitating, trains (3$\times$ at 40 or 100 Hz) of small amplitude (0.1–2 V) and brief (100 μs) shocks were sufficient to deliver a suprathreshold drive (Fig. 4*D* and *E*). Indeed, the small amplitudes of the first EPSP in the train (2.9 ± 2.0 mV, $n = 10$, burst mode, and 2.2 ± 1.2 mV, $n = 10$, tonic mode) suggested that our synaptic stimulations involved activation of only a few terminals. This finding that these small stimulations triggered AP bursts from hyperpolarized potentials suggested that dendritic T-channels boosted small numbers of synaptic inputs.

Global dendritic calcium accumulations during local synaptic excitation

We next examined the spatial propagation of local synaptic excitation, by measuring calcium accumulations on dendritic branches at three positions: adjacent to the stimulating electrode, at proximal dendritic segments of the same dendrite, and at a dendrite emerging from the other pole of the soma. We wondered if low threshold spikes synaptically triggered in burst mode could globally propagate like those triggered by somatic current injections (Fig. 2). Second, we wondered if the LTS could boost small synaptic inputs and explain the strength of unitary connections in LTS interneurones (Markram *et al.* 1998; Kozloski *et al.* 2001).

Burst mode. At hyperpolarized potentials ($V_m = -77.6 \pm 6.0$ mV, $n = 10$), we only observed calcium influx during the trains of synaptic stimulation that evoked low threshold spikes. Synaptically evoked low threshold spikes showed remarkably stereotyped calcium signals across cells. First, calcium influx was always time-locked to the LTS, and not to previous subthreshold synaptic excitation or LTS-triggered APs (Fig. 4*D*). Second, the LTS was always generated by the third shock, irrespective of train frequency ($n = 6/6$, 100 Hz; $n = 4/4$, 40 Hz) (Fig. 4*D*). Third, we repeatedly observed ($n = 5/5$) that low threshold spikes synaptically triggered at one pole of the cell could propagate through the soma and to a contralateral dendrite, over 100 μm from the stimulated dendritic segment (Fig. 4*D* and *E*). Lastly, the synaptically evoked LTS calcium accumulation was not different in amplitude from somatically generated LTS at matched dendritic sites (Fig. 4) ($(\Delta F/F_{\text{synaptic}})/(\Delta F/F_{\text{LTS,intrinsic}})$: distal, 1.03 ± 0.16; intermediate, 1.09 ± 0.32; proximal, 0.97 ± 0.10; soma, 0.71 ± 0.13; contralateral dendrite, 1.03 ± 0.08, $n = 5$). Thus, low threshold spikes produced stereotyped, global calcium signals independent of how and where they were generated. As in thalamic relay neurones, the LTS was recruited in an all-or-none fashion (Zhan *et al.* 1999), and the entire dendritic tree behaved as a single all-or-none spiking unit.

Tonic mode. Synaptic responsiveness at depolarized membrane potentials (58.0 ± 4.0 mV $n = 10$) differed from identical stimulation at hyperpolarized potentials in three fundamental ways. First, stimulations in tonic mode resulted in more precisely timed single action potentials 6.1 ± 4.0 ms after the second synaptic input, while in burst mode, APs were initiated with longer latency, 12.2 ± 6.2 ms, after the third synaptic input. We attribute this delay to the effct of the slow LTS-mediated depolarization. Second, calcium influxes in tonic mode were time-locked to sodium APs, and were similar in amplitude to those elicited by somatically

generated backpropagating APs at matched dendritic sites (Fig. 4*C* and *E*). Lastly, AP-associated calcium signals during synaptic stimulation in tonic mode were significantly smaller than LTS-associated calcium signals triggered in burst mode, at all distances from the soma ($(\Delta F/F_{\text{burst}})/(\Delta F/F_{\text{tonic}})$: distal, 0.23 ± 0.20, $P < 0.001$; intermediate, 0.18 ± 0.07, $P < 0.001$; proximal, 0.20 ± 0.10, $P < 0.001$; soma, 0.37 ± 0.16, $P < 0.05$; contralateral dendrite, 0.22 ± 0.07, $P < 0.001$).

However, just as in burst mode, the dendritic tree in tonic mode behaved as a single unit exhibiting global all-or-none calcium accumulations. We never observed local calcium signals or subthreshold calcium influx (multiple measurements in 10 cells). Thus, in contrast to pyramidal neurones and supragranular non-LTS interneurones, hyperpolarization increased synaptic calcium generation by establishing burst mode, consistent with the de-inactivation of T-type calcium channels

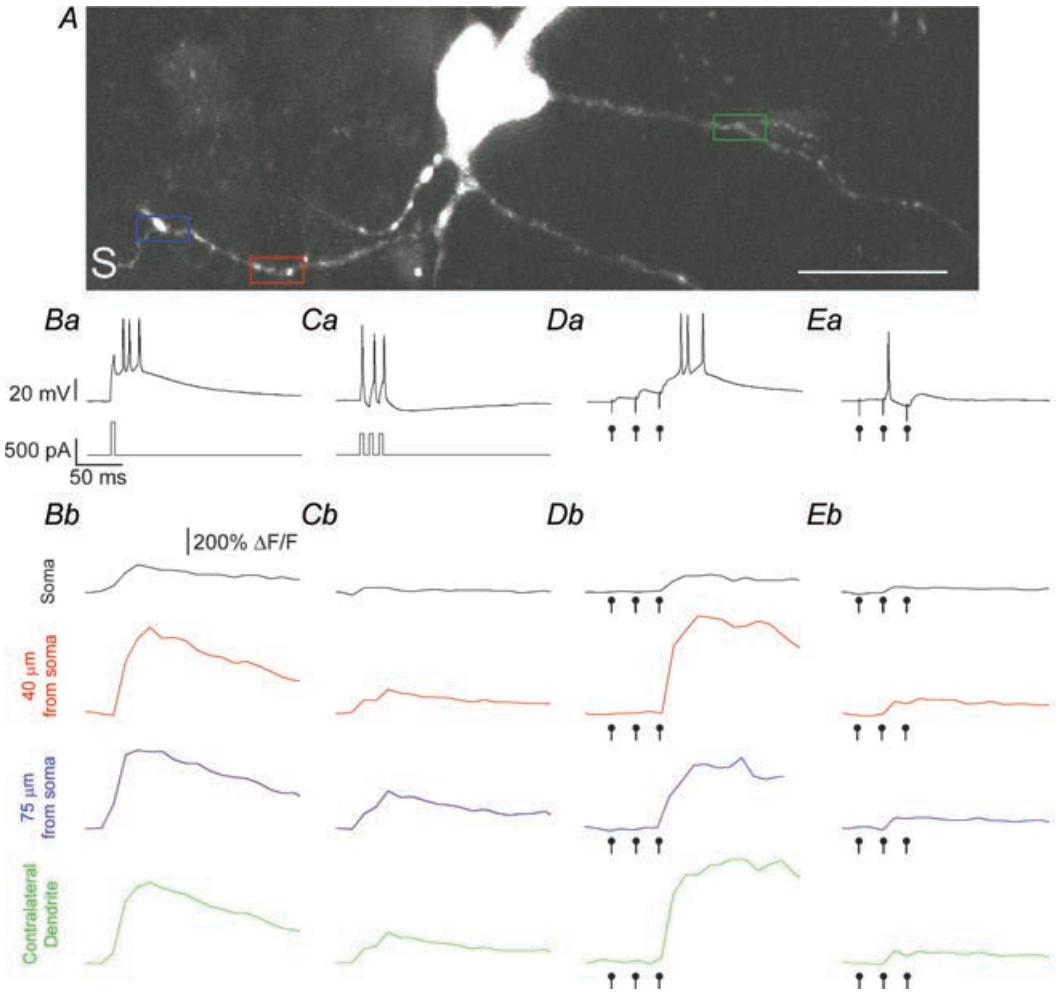

Figure 4. Global propagation of LTS evoked by local synaptic stimulation
A, *z*-projection of an LTS interneurone from layer 5 of primary somatosensory cortex. S marks the location of the stimulation electrode, which was always placed adjacent to terminal dendritic branches. Coloured boxes indicate the dendritic domains selected for line scan imaging at an additional 10× zoom (not shown). Scale bar = 20 μm. We systematically tested dendritic calcium responses throughout the dendritic tree. *Ba* and *Ca*, voltage response (top) to 5 ms somatic current injection (bottom) to a cell held at −78 mV (*B*), and −55 mV (*C*). *Bb* and *Cb*, calcium transients at the soma, and at three dendritic locations, as colour-coded in *A*. *Da* and *Ea*, synaptic response to a train of 3 stimulations (40 Hz) delivered at −78 mV (*D*) and −55 mV (*E*). Note how the LTS was triggered by the third stimulation when the cell was hyperpolarized. *Db* and *Eb*, calcium transients plotted as in *Bb* and *Cb* during synaptic stimulations. Dot markers indicate the timing of the synaptic stimulations. Note that the calcium influx was time-locked to the LTS in *D*, and to the AP in *E*. Also note that the magnitude of the synaptically evoked LTS was comparable to the somatically evoked LTS throughout the dendritic tree.

necessary for LTS burst generation (Fig. 2). In tonic mode, on the other hand, synaptically triggered sodium-based APs triggered global calcium accumulations.

LVA calcium channels recruited by AMPARs dominate synaptic calcium dynamics

As explained, in burst mode, calcium accumulations were indistinguishable during synaptically or intrinsically evoked LTS, even at activated distal dendrites. This was also the case for sodium-based APs in tonic mode. These observations, together with the fact that in burst mode we never observed calcium influx during synaptic stimulations subthreshold for low-threshold spikes, suggested that during our stimulation protocol, calcium influx in LTS cell dendrites is triggered mostly by calcium channels, and not by glutamate-gated calcium-permeable channels.

Consistent with this, blockade of NMDARs with D-APV had no effect on the calcium signal or on the physiological response to stimulation (Fig. 6*A*). This finding was in stark contrast to pyramidal neurones and supragranular interneurones, where NMDA receptor activation dominates subthreshold calcium influx (Yuste *et al.* 1999; Kovalchuk *et al.* 2000; Schiller *et al.* 2000; Goldberg *et al.* 2003*c*).

Our failure to observe any local calcium accumulations suggested that the entire dendritic tree of LTS cells cooperates in all-or-none calcium signalling. One mechanism for all-or-none global calcium accumulations during local synaptic excitation could be a global calcium release from internal stores (Ludwig *et al.* 2002). We tested this by performing experiments in the presence of CPA, a drug which blocks intracellular release of calcium by inhibiting the SERCA pump. CPA had no effect on synaptically evoked calcium signals at any dendritic site examined (Fig. 6*B*).

Another explanation for the global calcium signals observed during local synaptic stimulation is that low threshold spikes regeneratively propagated through the dendritic tree, as in Fig. 2. We tested for this LVA calcium channel-mediated globalization of calcium influx by performing experiments in the presence of 20 μM Ni^{2+}. First, we found that low nickel did not significantly affect synaptic transmission. The amplitude of the 2nd EPSP was not different in control *versus* nickel conditions (control 2nd EPSP = 3.9 ± 0.6; nickel 2nd EPSP = 4.9 ± 2.2 mV) (Fig. 6*C*). However, low nickel specifically reduced the

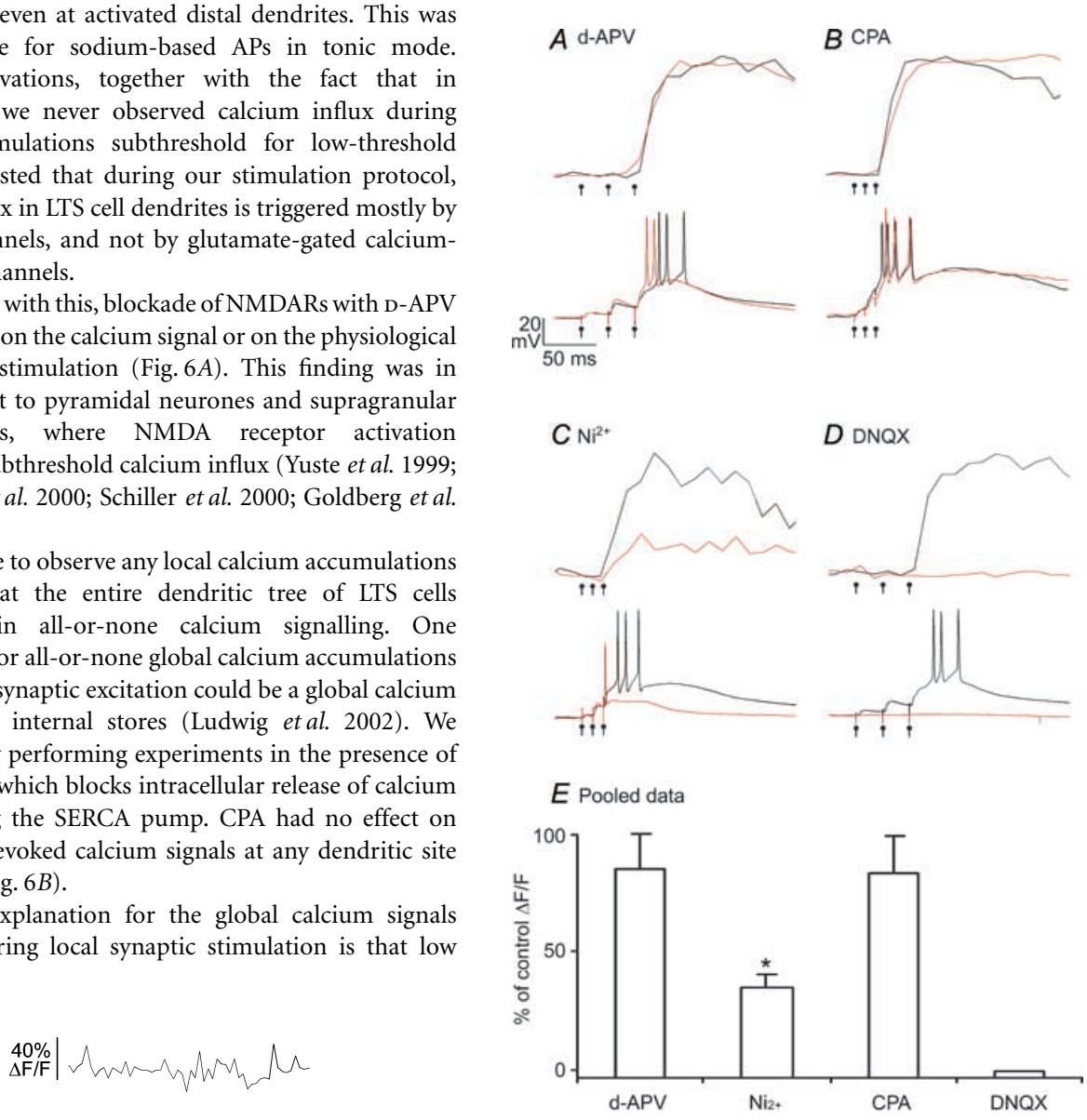

Figure 6. AMPA receptor driven depolarization recruits low threshold spikes to trigger global synaptic calcium events
Calcium transients during local synaptic stimulation are plotted above synaptically evoked EPSPs in control (black) conditions and in the presence of 100 μM D-APV (*A*), 30 μM CPA (*B*), 20 μM nickel (*C*), and DNQX (*D*). *E*, data pooled from D-APV ($n = 4$), nickel ($n = 3$), CPA ($n = 3$) and DNQX ($n = 3$) experiments. Calcium transients were from the distal (> 80 μm) dendrites adjacent to the stimulation electrode.

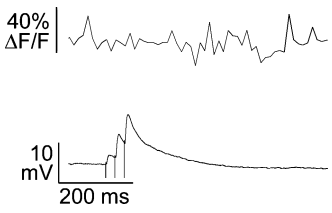

Figure 5. Subthreshold EPSP trains do not evoke calcium signals
Top, $\Delta F/F$ transient taken from distal dendrite immediately adjacent to the stimulation electrode. Bottom, synaptic response to a train of shocks (3 delivered at 40 Hz). Cell was held at −78 mV.

low threshold spike and its associated calcium influx, at all dendritic sites, indicating that LVA channels triggered synaptic low threshold spikes which propagated throughout the dendritic tree.

Given the dramatic effect that T-channels had on triggering large, global calcium accumulations during local synaptic excitation in burst mode, we wondered how they were recruited. Since NMDAR activation was not significant in either burst or tonic modes, we suspected that AMPA receptor-mediated depolarization may recruit sodium spikes, in tonic mode, and LVA calcium channels, in burst mode. In the presence of DNQX (20 μM), to block non-NMDA ionotropic glutamate receptors, both EPSPs and synaptic calcium influx were totally blocked (Fig. 6*D*). Thus, we conclude that in burst mode, synaptic calcium influx proceeded via AMPA-mediated recruitment of T-type calcium channels, which then propagated throughout the dendritic tree to trigger global calcium influx and a burst of APs. In tonic mode, the majority of T-type calcium channels are inactivated, and AMPAR-mediated depolarization directly triggers global APs.

Discussion

We have examined the dendritic calcium dynamics in low threshold spiking (LTS) interneurones in layer 5 of mouse visual and somatosensory cortices. In both cortical regions, somatostatin-positive LTS cells were Martinotti cells, with local dendritic arborization in layer 5 and dense axonal innervation of layer 1. We found that their intrinsic and synaptic behaviour depended on the firing mode, and thus the membrane potential. In tonic mode (>-60 mV), sodium-based action potentials actively backpropagated into the dendritic tree and caused instantaneous calcium accumulations. In burst mode (<-70 mV), low threshold spikes triggered by T-type calcium channels also regeneratively propagated through the dendritic tree and dominated intrinsic dendritic calcium dynamics, especially at distal sites. The crucial difference between the two modes, therfore, is the availability of the T-type calcium channel, which is inactivated at more depolarized potentials (Crunelli *et al.* 1989). Importantly, small synaptic inputs were able to trigger bursts by activating I_T, and endowing the LTS interneurone with heightened sensitivity to small numbers of presynaptic pyramids even at hyperpolarized membrane potentials, far from sodium channel threshold. Our findings thus explain the suprathreshold activation of LTS cells by individual pyramidal neurones in previous studies (Markram *et al.* 1998; Kozloski *et al.* 2001).

During facilitating trains of synaptic input, the entire LTS dendritic tree behaved as a single non-linear subunit, generating global calcium signals during suprathreshold trials. In contrast to cortical pyramids and diverse classes of supragranular non-LTS cells, which exhibit calcium compartmentalization during subthreshold activation (Schiller *et al.* 2000; Wei *et al.* 2001; Goldberg *et al.* 2003*c*), LTS interneurones express differential calcium dynamics established by the inactivation state of dendritic T-type calcium channels (Fig. 4). LTS interneurones possessed two thresholds: in tonic mode, the threshold for single APs was set by sodium channels, while in burst mode, the threshold for the LTS, and thus AP bursts, was set by T-channels.

Low threshold spikes dominate intrinsic dendritic calcium dynamics

In addition to subserving distinct membrane potential-dependent firing modes, LTS interneurones exhibit state-dependent calcium signalling. LTS interneurones generated rebound bursts after release from hyperpolarization (Fig. 1), implicating T-type calcium channels (Crunelli *et al.* 1989; Kim *et al.* 2001). Recent evidence suggests that R-type calcium channels share with T-channels micromolar sensitivity to nickel blockade, and activation and deactivation kinetics at subthreshold potentials (Foehring *et al.* 2000; Sochivko *et al.* 2003). However, unlike T-type calcium channels, R-type calcium channels are not significantly activated at more negative potentials than -60 mV (Randall & Tsien, 1997; Foehring *et al.* 2000), and thus would not trigger the rebound bursts which define the LTS interneurone phenotype (Fig. 1). Thus, while T-type calcium channels trigger low threshold spikes, other calcium channel subtypes including R- and L-type channels may be subsequently recruited and contribute to total calcium influx.

The dominance of low threshold spikes on dendritic calcium dynamics, especially at distal dendritic sites, represents the first direct demonstration that low-voltage-activated calcium channels are expressed at high densities on dendrites of cortical LTS interneurones. Moreover, LVA calcium channels appeared to be expressed at higher densities on distal dendrites (Fig. 2). This strategic placement of these calcium channels to interact preferentially with synaptic inputs may be a general principle in neurones throughout the CNS which operate in burst and tonic modes (Destexhe *et al.* 1998; Sherman, 2001). Further, since low threshold bursts can be triggered by small voltage deflections from hyperpolarized membrane potentials, dendritic T-channels may endow

LTS interneurones with suprathreshold sensitivity to single presynaptic pyramidal inputs (Markram *et al.* 1998; Kozloski *et al.* 2001).

The intrinsic calcium dynamics of LTS interneurones were dramatically different not only from pyramidal neurones but also from other interneurone subclasses. First, the firing mode of the cell, determined by the membrane potential and thus the level of background activity, radically determined the amplitude and spatial distribution of dendritic calcium (Fig. 2). Second, single APs and AP trains invaded vast territories of the dendritic tree without significant decrement (Fig. 2*D*–*G*). This finding was in contrast to fast-spiking and irregular-spiking supragranular interneurones and CA1 pyramidal neurones, where Ia type potassium currents restrict AP propagation from distal dendrites (Hoffman *et al.* 1997; Goldberg *et al.* 2002. 2003*b*; Frick *et al.* 2003). These results highlight the diversity of intrinsic calcium signalling in distinct classes of interneurones, and shows that calcium dynamics in interneurone dendrites varies across interneurone populations.

Firing mode determines synaptic responsiveness and calcium dynamics

Low threshold spikes generated from hyperpolarized potentials triggered a burst of APs and large amplitude calcium signals at all dendritic sites. In tonic mode, synaptic stimulation evoked precisely timed single APs and smaller but global calcium signals (Fig. 4). This cell-to-cell homogeneity in this state dependence was perhaps the most remarkable characteristic of LTS interneuronal synaptic responsiveness. Whereas in LII/III we observed heterogeneity in mechanism and spatial distribution of calcium influx within interneuronal subclasses, LTS cells behaved identically. First, in burst mode, low threshold spikes always provided sufficient depolarization to recruit bursts of sodium-based action potentials, and in tonic mode, calcium signals only occurred during and were time-locked to APs. Thus we did not observe subthreshold calcium influx (Figs 1 and 4). Second, calcium signals generated by either low threshold spikes in burst mode or by APs in tonic mode were observed at all dendritic sites tested. Third, in both firing modes, the method of stimulation (somatic current injection or local synaptic excitation of a distal dendrite) did not effect the amplitude or spatial distribution calcium accumulations. Lastly, we found that single spikes generated in tonic mode always occurred precisely after the second synaptic stimulation, while low threshold spikes in burst mode occurred after the third. Thus LTS interneurones behaved reliably during a stereotyped stimulation protocol.

Global synaptic calcium signalling during local synaptic excitation

In pyramids and supragranular interneurones, NMDA receptor activation dominates dendritic calcium influx, and dendritic morphological complexity operates in tandem with local conductances to functionally compartmentalize convergent synaptic inputs (Schiller *et al.* 2000; Wei *et al.* 2001; Goldberg *et al.* 2002, 2003*c*). In contrast, in LTS cells, D-APV had no effect on EPSPs, LTS generation, or synaptic calcium signals (Fig. 6*A* and *B*). CPA also had no effect, while DNQX blocked EPSPs and calcium signals. Importantly, nickel (20 μM) significantly reduced both the LTS and its associated calcium signal, indicating the intrinsically and synaptically evoked low threshold spikes depended on LVA calcium channels.

Thus, voltage-gated calcium channels, recruited regeneratively by either low threshold spikes or sodium based APs, constituted the major source of synaptic calcium entry, ensuring that the entire dendritic tree of LTS cells operated as a single state-dependent all-or-none signalling domain (Fig. 4).

This unique handling of calcium suggests a wholly distinct function of calcium in these dendrites. While NMDAR-dependent compartmentalized calcium signals may subserve synaptic coincidence detection and plasticity in other cell types, we propose that calcium in LTS cells acts to homeostatically stabilize firing modes, and thus the cell's output regime. Consistent with this hypothesis, in dopaminergic midbrain neurones, which also operate in burst and tonic firing modes, T-channels are selectively coupled to calcium-activated potassium currents (Wolfart & Roeper, 2002). Also, in supragranular SST interneurones, calcium triggers exocytotic GABA release, which causes a depression in the activity of presynaptic terminals (Zilberter *et al.* 1999). Both of these calcium-dependent mechanisms reduce excitability and would increase T-channel deinactivation after bursts. Thus, through either of these mechanisms, global calcium signals during suprathreshold activity in LTS interneurones could act to maintain the burst mode, even during high levels of afferent activity.

The function of LTS Martinotti cells in neocortical circuits: burst detection and control

Excitatory inputs to layer 1 include cortico-cortical projections as well as fibres from intralaminar thalamic nuclei, both of which may subserve 'top-down' cortical feedback (Llinás, 2002). Deep layer pyramidal neurones appear specially designed to integrate this input with the activation of lower layers: excitatory synaptic activation

of the distal apical tuft of pyramidal neurones, located in layer 1, generates distal calcium spikes, which in turn trigger AP bursts when coupled with proximal excitation in lower layers (Yuste *et al.* 1994; Larkum *et al.* 1999; Larkum *et al.* 2001). These layer 5 cells project to lower layer SST interneurones (Kozloski *et al.* 2001), and the strong facilitation of excitatory inputs we observed on LTS cells indicates that LTS cells are particularly sensitive to bursts of layer 5 pyramidal neurones, to the point that they can fire in response to a single axon (Markram *et al.* 1998; Kozloski *et al.* 2001). It is not a coincidence that the axonal plexus of LTS cells targets the very site where bursts are generated in their afferent population. Thus, deep layer LTS Martinotti cells are at once perfectly situated to both detect and control bursting of pyramidal neurones. Since we found no detectable difference in their behaviour in visual and somatosensory cortices, and since they are also expressed in frontal cortex (Kawaguchi & Kubota, 1996), we propose that infragranular LTS interneurones control deep layer bursting across neocortex. Like in the hippocampus (Buhl *et al.* 1994), the axonal targeting of neocortical interneurones could be matched to control specific subcellular domains of pyramidal cells.

References

Abeles M (1991). *Corticonics*. Cambrdige University Press, Cambridge, England.

Amitai Y, Gibson JR, Beierlein M, Patrick SL, Ho AM, Connors BW & Golomb D (2002). The spatial dimensions of electrically coupled networks of interneurons in the neocortex. *J Neurosci* **22**, 4142–4152.

Angulo MC, Rossier J & Audinat E (1999). Postsynaptic glutamate receptors and integrative properties of fast-spiking interneurons in the rat neocortex. *J Neurophysiol* **82**, 1295–1302.

Beierlein M, Gibson JR & Connors BW (2000). A network of electrically coupled interneurons drives synchronized inhibition in neocortex. *Nat Neurosci* **3**, 904–910.

Beierlein M, Gibson JR & Connors BW (2003). Two dynamically distinct inhibitory networks in layer 4 of the neocortex. *J Neurophysiol* **90**, 2987–3000.

Braitenberg V & Schüzt A (1991). *Anatomy of the Cortex*. Springer, Berlin.

Buhl EH, Halasy K & Somogyi P (1994). Diverse sources of hippocampal unitary inhibitory postynaptic potentials and the number of synaptic release sites. *Nature* **368**, 823–828.

Cajal S Ramón y (1899). *Textura del Sistema Nervioso del Hombre y de los Vertebrados*. N. Moya, Madrid.

Cauli B, Audinat E, Lambolez B, Angulo MC, Ropert N, Tsuzuki K, Hestrin S & Rossier J (1997). Molecular and physiological diversity of cortical nonpyramidal cells. *J Neurosci* **17**, 3894–3906.

Crunelli V, Lightowler S & Pollard CE (1989). A T-type Ca^{2+} current underlies low-threshold Ca^{2+} potentials in cells of the cat and rat lateral geniculate nucleus. *J Physiol* **413**, 543–561.

Deans MR, Gibson JR, Sellitto C, Connors BW & Paul DL (2001). Synchronous activity of inhibitory networks in neocortex requires electrical synapses containing connexin36. *Neuron* **31**, 477–485.

Destexhe A, Neubig M, Ulrich D & Huguenard J (1998). Dendritic low-threshold calcium currents in thalamic relay cells. *J Neurosci* **18**, 3574–3588.

Fairen A, De Felipe J & Regidor J (1984). Nonpyramidal neurons. In *Cerebral Cortex*,vol. 1, ed. Peters A & Jones EG., pp. 201–253. Plenum, New York.

Foehring RC, Mermelstein PG, Song WJ, Ulrich S & Surmeier DJ (2000). Unique properties of R-type calcium currents in neocortical and neostriatal neurons. *J Neurophysiol* **84**, 2225–2236.

Fox AP, Nowycky MC & Tsien RW (1987). Kinetic and pharmacological properties distinguishing three types of calcium currents in chick sensory neurones. *J Physiol* **394**, 149–172.

Frick A, Magee J, Koester HJ, Migliore M & Johnston D (2003). Normalization of Ca^{2+} signals by small oblique dendrites of CA1 pyramidal neurons. *J Neurosci* **23**, 3243–3250.

Fricker D & Miles R (2000). EPSP amplification and the precision of spike timing in hippocampal neurons. *Neuron* **28**, 559–569.

Gee CE, Woodhall G & Lacaille JC (2001). Synaptically activated calcium responses in dendrites of hippocampal oriens-alveus interneurons. *J Neurophysiol* **85**, 1603–1613.

Gibson JR, Beierlein M & Connors BW (1999). Two networks of electrically coupled inhibitory neurons in neocortex. *Nature* **402**, 75–79.

Goldberg J, Holthoff K & Yuste R (2002). A problem with Hebb and local spikes. *Trends Neurosci* **25**, 433–435.

Goldberg JH, Tamas G, Aronov D & Yuste R (2003*a*). Calcium microdomains in aspiny dendrites. *Neuron* **40**, 807–821.

Goldberg JH, Tamas G & Yuste R (2003*b*). Ca^{2+} imaging of mouse neocortical interneurone dendrites: Ia-type K^{+} channels control action potential backpropagation. *J Physiol* **551**, 49–65.

Goldberg JH, Yuste R & Tamas G (2003*c*). Ca^{2+} imaging of mouse neocortical interneurone dendrites: contribution of Ca^{2+}-permeable AMPA and NMDA receptors to subthreshold Ca^{2+} dynamics. *J Physiol* **551**, 67–78.

Hermsmeyer K (1998). Role of T channels in cardiovascular function. *Cardiology* **89** (Suppl. 1), 2–9.

Hoffman DA, Magee JC, Colbert CM & Johnston D (1997). Potassium channel regulation of signal propagation in dendrites of hippocampal pyramidal neurons. *Nature* **387**, 869–875.

Jahnsen H & Llinas R (1984). Voltage-dependent burst-to-tonic switching of thalamic cell activity: an in vitro study. *Arch Ital Biol* **122**, 73–82.

Johnston D, Magee JC, Colbert CM & Christie BR (1996). Active properties of neuronal dendrites. *Ann Rev Neurosci* **19**, 165–186.

Kaiser KM, Lubke J, Zilberter Y & Sakmann B (2004). Postsynaptic calcium influx at single synaptic contacts between pyramidal neurons and bitufted interneurons in layer 2/3 of rat neocortex is enhanced by backpropagating action potentials. *J Neurosci* **24**, 1319–1329.

Kaiser KM, Zilberter Y & Sakmann B (2001). Back-propagating action potentials mediate calcium signalling in dendrites of bitufted interneurons in layer 2/3 of rat somatosensory cortex. *J Physiol* **535**, 17–31.

Kawaguchi Y & Kondo S (2002). Parvalbumin, somatostatin and cholecystokinin as chemical markers for specific GABAergic interneuron types in the rat frontal cortex. *J Neurocytol* **31**, 277–287.

Kawaguchi Y & Kubota Y (1996). Physiological and morphological identification of somatostatin- or vasoactive intestinal polypeptide-containing cells among GABAergic cell subtypes in rat frontal cortex. *J Neurosci* **16**, 2701–2715.

Kim D, Song I, Keum S, Lee T, Jeong MJ, Kim SS, McEnery MW & Shin HS (2001). Lack of the burst firing of thalamocortical relay neurons and resistance to absence seizures in mice lacking alpha$_{1G}$ T-type Ca^{2+} channels. *Neuron* **31**, 35–45.

Kovalchuk Y, Eilers J, Lisman J & Konnerth A (2000). NMDA receptor-mediated subthreshold Ca^{2+} signals in spines of hippocampal neurons. *J Neurosci* **20**, 1791–1799.

Kozloski J, Hamzei-Sichani F & Yuste R (2001). Stereotyped position of local synaptic targets in neocortex. *Science* **293**, 868–872.

Larkum M, Zhu J & Sakmann B (1999). A new cellular mechanism for coupling inputs arriving at different cortical layers. *Nature* **398**, 338–341.

Larkum ME, Zhu JJ & Sakmann B (2001). Dendritic mechanisms underlying the coupling of the dendritic with the axonal action potential initiation zone of adult rat layer 5 pyramidal neurons. *J Physiol* **533**, 447–466.

Llinás R (2002). *I of the vortex: From Neurons to Self*. MIT Press, Cambridge, MA, USA.

Lorente De Nó R (1922). La corteza cerebral del ratón. *Trab Laboratory Invest Bio (Madrid)* **20**, 41–78.

Ludwig M, Sabatier N, Bull PM, Landgraf R, Dayanithi G & Leng G (2002). Intracellular calcium stores regulate activity-dependent neuropeptide release from dendrites. *Nature* **418**, 85–89.

Majewska A, Yiu G & Yuste R (2000). A custom-made two-photon microscope and deconvolution system. *Pflugers Arch* **441**, 398–409.

Markram H, Wang Y & Tsodyks M (1998). Differential signaling via the same axon of neocortical pyramidal neurons. *Proc Natl Acad Sci U S A* **95**, 5323–5328.

Martina M, Vida I & Jonas P (2000). Distal initiation and active propagation of action potentials in interneuron dendrites. *Science* **287**, 295–300.

Miles R & Wong RKS (1983). Single neurones can initiate synchronized population discharge in the hippocampus. *Nature* **306**, 371–373.

Porter JT, Cauli B, Staiger JF, Lambolez B, Rossier J & Audinat E (1998). Properties of bipolar VIPergic interneurons and their excitation by pyramidal neurons in the rat neocortex. *Eur J Neurosci* **10**, 3617–3628.

Randall AD & Tsien RW (1997). Contrasting biophysical and pharmacological properties of T-type and R-type calcium channels. *Neuropharmacology* **36**, 879–893.

Reyes A, Lujan R, Rozov A, Burnashev N, Somogyi P & Sakmann B (1998). Target-cell-specific facilitation and depression in neocortical circuits. *Nat Neurosci* **1**, 279–285.

Rolls ET & Treves A (1998). *Neural Networks and Brain Function*. Oxford University Press, Oxford.

Rozov A, Jerecic J, Sakmann B & Burnashev N (2001). AMPA receptor channels with long-lasting desensitization in bipolar interneurons contribute to synaptic depression in a novel feedback circuit in layer 2/3 of rat neocortex. *J Neurosci* **21**, 8062–8071.

Rozsa B, Zelles T, Vizi ES & Lendvai B (2004). Distance-dependent scaling of calcium transients evoked by backpropagating spikes and synaptic activity in dendrites of hippocampal interneurons. *J Neurosci* **24**, 661–670.

Ruiz-Marcos A & Valverde F (1970). Dynamic architecture of the visual cortex. *Brain Res* **19**, 25–39.

Schiller J, Major G, Koester HJ & Schiller Y (2000). NMDA spikes in basal dendrites of cortical pyramidal neurons. *Nature* **404**, 285–289.

Sherman SM (2001). Tonic and burst firing: dual modes of thalamocortical relay. *Trends Neurosci* **24**, 122–126.

Sochivko D, Chen J, Becker A & Beck H (2003). Blocker-resistant Ca^{2+} currents in rat CA1 hippocampal pyramidal neurons. *Neuroscience* **116**, 629–638.

Wei DS, Mei YA, Bagal A, Kao JP, Thompson SM & Tang CM (2001). Compartmentalized and binary behavior of terminal dendrites in hippocampal pyramidal neurons. *Science* **293**, 2272–2275.

Wolfart J & Roeper J (2002). Selective coupling of T-type calcium channels to SK potassium channels prevents intrinsic bursting in dopaminergic midbrain neurons. *J Neurosci* **22**, 3404–3413.

Yuste R, Gutnick MJ, Saar D, Delaney KD & Tank DW (1994). Calcium accumulations in dendrites from neocortical neurons: an apical band and evidence for functional compartments. *Neuron* **13**, 23–43.

Yuste R, Majewska A, Cash S & Denk W (1999). Mechanisms of calcium influx into spines: Heterogeinity among spines, coincidence detection by NMDA receptors and optical quantal analysis. *J Neurosci* **19**, 1976–1987.

Yuste R & Tank DW (1996). Dendritic integration in mammalian neurons, a century after Cajal. *Neuron* **16**, 701–716.

Zhan XJ, Cox CL, Rinzel J & Sherman SM (1999). Current clamp and modeling studies of low-threshold calcium spikes in cells of the cat's lateral geniculate nucleus. *J Neurophysiol* **81**, 2360–2373.

Zilberter Y, Kaiser KM & Sakmann B (1999). Dendritic GABA release depresses excitatory transmission between layer 2/3 pyramidal and bitufted neurons in rat neocortex. *Neuron* **24**, 979–988.

Acknowledgements

The study was funded by the NEI (EY11787), NINDS (N540726), the New York STAR Center for High Resolution Imaging of Functional Neural Circuits and the John Merck Fund.

Supplementary material

The online version of this paper can be found at:
DOI: 10.1113/jphysiol.2004.064519
http://jp.physoc.org/cgi/content/full/jphysiol.2004.064519v1/DC1
and contains supplementary material entitled: Sustained hyperpolarization and brief depolarizations from hyperpolarized potentials trigger low threshold spikes.
This material is also available at:
http://www.blackwellpublishing.com/products/journals/suppmat/tjp337/tjp337sm.htm